Porous 3D Polymers for High Pressure Methane Storage and Carbon Dioxide Capture

Silvia Bracco, Daniele Piga, Irene Bassanetti, Jacopo Perego, Angiolina Comotti* and Piero Sozzani*

Department of Materials Science, University of Milano Bicocca, Via R. Cozzi 55, 20125 Milan, Italy.

ABSTRACT:

High surface area 3D polymers represent one of the most promising classes of porous materials because of their high gas uptake and stability to thermal and chemical degradation. A series of porous organic polymers with aromatic building units have been synthetized and compared to explore their high pressure performance as absorbents of gases of relevant importance for energy and the environment. Particular attention was paid to methane storage up to pressures as high as 180 and ambient temperature. Porous polymers were prepared starting from a wide choice of spatially expanded aromatic monomers: a systematic change in the number of rings, variable size and shape were taken under consideration. The high number of rings (up to 6), which act as multiple reactive sites and form a number of connections between the multi-dentate nodes, result in an extensive cross-linked framework. Condensation was obtained by two alternative synthetic routes, viz., Yamamoto cross-coupling and Friedel Crafts alkylation reactions. The structural characteristics and high stability of the porous polymers, even to mechanical compression, were carefully determined by several methods, including 1D and 2D solid state NMR, FT IR and thermal analyses. The CH_4 uptake in the porous polymers, allowed an understanding of the incremental response to pressure, up to extremely high values, and the exploitation of the extensive pressure range to customize the gas absorption/desorption cycles for storage and transportation. The excellent chemical resistance and the high thermal stability, together with scalability and low cost, are key factors for future applications. Owing to the notable presence of large mesopores and network flexibility, combined with high surface area, a remarkable gain at high pressure was achieved, ensuring a highly competitive uptake/delivery efficiency. CO_2 and N_2 adsorption isotherms collected at room temperature enabled the assessment of the suitability of such polymer networks for CO_2 selective separation and capture. In summary, the in-depth and extensive comparative screening within this class of materials up to high pressures provides the necessary parameters for further synthetic and applicative work.

INTRODUCTION

The need for alternative fuels is a key issue in our society, and methane, or natural gas, is a viable choice as a readily available option with a low carbon emission. However, current natural gas delivery methods, such as pipeline and liquid natural gas (LNG) technologies, can prove unsatisfactory for political and economic reasons.[1] This is particularly the case for gas reservoirs which are often located off-shore: natural gas is present in quantities that typically do not justify capital-intensive infrastructural investment, such as that necessary to build new pipelines or liquefaction/regasification facilities. Therefore, keen interest has nourished Compressed Natural Gas (CNG) technology.[2] In CNG applications, whether terrestrial or marine, natural gas is compressed up to high pressures for storage and transportation inside appropriate CNG containment systems. CNG is also applied in several other industrial sectors including the wide automotive field.[2]

Storage of natural gas in highly porous materials, also known as Adsorbed Natural Gas (ANG), has been proposed, as an innovative way to store and transport large amounts of natural gas. Such porous materials include the widely described zeolites, activated carbons and metal organic frameworks (MOFs)[3] but in some cases there are limitations, *in primis* thermal and chemical stability.[4] In existing metal-organic compounds, although high CH_4 uptake is observed,[5] positively charged metal atoms bound to electron-rich organic ligands can be sensitive in the long term to polar substances, such as water, that could contaminate and degrade the material during its life-time.[6] In addition, uptake measurements are frequently limited to moderate pressures, such as 35 or 65 bar, adequate for vehicular applications. Consequently, there remains a need for high pressure methane storage materials, which would improve their performance for general uses.

Porous organic polymers offer a valid option as the carbon-carbon bond connectivity of such polymers imparts high thermal and chemical stability, resistance to contaminants and low water affinity. Indeed, a number of them endowed with high surface areas and pore volumes, have been proposed in recent years for gas capture and storage.[7] For optimal high-pressure performance the contribution of mesopores must be significant, and high deliverable capacity is achieved only if a moderate amount of gas is retained at low pressure during the discharge step.[8] Porous 3D polymers are endowed with a complete range of pore size (from subnano to tenths of nanometers) and can fulfill these requisites, thus, they are promising candidates for an efficient storage and delivery. Furthermore, in 3D cross-linked polymeric networks with a random number of connections between nodes, high pressure capacity can be improved by framework flexibility and expandability.[9] To date, for this family of materials, methane capture has been investigated only in a limited number of reports[10] and CH_4 absorption and storage at high pressures (up to 180 bar) in porous organic polymers has not yet been explored.

The present research activity focused on the synthesis and methane uptake/release over a wide range of pressures, up to 180 bar, of high-surface-area porous materials with carbon-carbon covalent bonds connecting the aromatic rings. Two synthetic routes were pursued: Yamamoto-coupling and Friedel-Crafts alkylation (FC) reactions. The monomers possess a high number of aromatic rings and multiple reactive sites which connect with other monomers to form multiple links, resulting in an extensive cross-linked framework in which each monomeric unit is bound to more than two other monomeric units (Figure 1). A systematic variation of the connectivity and geometry of monomer units allowed the investigation of the influence of polymer structure on gas adsorption properties up to high pressures. A number of new monomers and synthetic conditions were explored to compare methane adsorption for a wide collection of aromatic porous networks, thus providing efficiency and convenience parameters for these materials.

The porous materials were characterized by several techniques, including N_2 adsorption isotherms, thermal analysis and solid state 1D and 2D NMR, in order to extract information about their gas capacity, thermal stability and structure. CH_4 isotherms show a moderate slope in the initial part, followed by a continuous increase in uptake at higher pressures, leading to a high storage efficiency. It is to be noted that the production scalability and the low-cost of the synthetic procedure using inexpensive catalysts, makes this family of porous products particularly suitable for practical purposes. Moreover, evidence of selective CO_2 adsorption, at room temperature and 10 bar over N_2, enforces the utility of the present extensive screening, also for CO_2 capture and separation for cleaner combustion processes.

EXPERIMENTAL SECTION

General Procedure for the Friedel-Craft reactions. Formaldehyde dimethyl acetal (FDA) and anhydrous $FeCl_3$ were added to a solution of monomer in 1,2-dichloroethane, under inert gas atmosphere. The mixture was then stirred at 80°C for 24 hours in a double-necked flask equipped with a cooling vapor condenser. After the reaction, the resulting powder was collected by filtration and then washed with methanol several times, until the filtrating liquor was colorless. The product was purified, by Soxhlet extraction by methanol for 48 hours and subsequently dried under vacuum (10^{-3} torr) at 130 °C for 15 hours. The monomer:FDA:$FeCl_3$ molar ratios are as follows, 1:4:4 for trans-stilbene, 1:6:6 for tripticene, 1:8:8 for 9,9'-spirobifluorene, rubrene and 4,4'-di(9H-carbazol-9-yl)biphenyl, 1:12:12 for hexaphenylbenzene, hexaphenyldisilane and hexaphenylcyclotrisiloxane. The purity of the monomers was > 99%.

General Procedure for the Yamamoto reactions. The 5,10,15,20-tetrakis(4-bromophenyl)porphyrin monomer was purchased by Frontier Scientific. The 1,4-bis(3,6-dibromo-9H-carbazol-9-yl)benzene and the 4,4'-bis(3,6-dibromo-9H-carbazol-9-yl)biphenyl were obtained by bromuration of the precursors with N-bromosuccinimmide in THF at 40°C (1:3.5 ratio). Tetraphenylmethane was reacted with elemental Br_2 at room temperature for 12 hours. The product was crystallized twice to yield tetrakis(4-bromophenyl)methane (purity > 99%, by ^{1}H NMR).

The catalytic complex was prepared by adding bis(1,5-cyclooctadiene)nickel(0) ($Ni(COD)_2$) to 2,2'-bipyridyl and cis,cis-1,5-cyclooctadiene (COD) in dry DMF and THF solution. The porous polymers were obtained by adding dropwise the brominated monomer, dissolved in THF, to the catalytic mixture, under inert atmosphere, and the resulting mixture was stirred at 60 °C for 22 hours and at room temperature for 22 hours. The reaction was then quenched adding concentrated HCl (30 ml), until the solution turned green with a white suspension. The filtered product was washed with THF (2 x 100 ml), water (2 x 100 ml) and chloroform (2 x 100 ml) and dried in vacuum (10^{-3} torr) at 200°C. For further details see Tables S1 and S2.

The copolymer was obtained starting from a mixture of tetrakis(4-bromophenyl)methane and 5,10,15,20-betrakis(4-bromophenyl)porphyrin (80:20 ratio). The mixture was dissolved in dry THF, and was added dropwise to the catalytic mixture, under inert atmosphere, and stirred for 48 hours at 0°C. After the quenching, the copolymer was recovered as described above.

Characterization. Thermal stability was determined from a thermogravimetric analysis over a temperature range from 30 to 800 °C under air with a heating rate of 10°C/min. The weight loss was measured at 800°C. FT IR spectra were collected in transmission on an JASCO 4100 spectrometer using KBr disks.

^{13}C solid state NMR spectra were run at 75.5 MHz on a Bruker Avance 300 instrument operating at a static field of 7.04 T equipped with a 4 mm double resonance MAS probe. The samples were spun at magic angle at a spinning speed of 12.5 kHz, and ramped amplitude cross-polarization (RAMPCP) transfer of magnetization was applied. The 90° pulse for the proton was 2.9 μs. The ^{13}C cross polarization (CP) MAS experiments were run at 298 K using a contact times of 2 ms and a recycle delay of 6 s. ^{13}C single-pulse excitation (SPE) experiments with dipolar decoupling from hydrogen were run using a recycle delay of 60 s. The 90° pulse for carbon was 4.6 μs. Crystalline polyethylene was taken as an external reference at 32.8 ppm from TMS.

Phase-modulated Lee−Goldburg (PMLG) heteronuclear ^{1}H-^{13}C correlation (HETCOR) experiments coupled with fast magic angle spinning allowed the recording of the 2D spectra with a high resolution in hydrogen and carbon dimensions.[11] Narrow hydrogen resonances, with line widths on the order of 1−2 ppm, were obtained with homonuclear decoupling during t1. This resolution permits a sufficiently accurate determination of the proton species present in the system. The 2D PMLG ^{1}H-^{13}C HETCOR spectra were run with an LG period of 18.9 μs. The efficient transfer of magnetization to the carbon nuclei was performed by applying the RAMP-CP sequence. The cross-polarization times of 50 μs, 500 μs, 1 ms and 2 ms were applied. Quadrature detection in t_1 was achieved by the time proportional phase increments method (TPPI). The carbon signals were acquired during t_2 under proton decoupling by applying the two-pulse phase modulation scheme (TPPM). The 2D experiments were conducted at 298 K under magic-angle spinning (MAS) conditions at 12.5 kHz.

Nitrogen and carbon dioxide adsorption isotherms. N_2 adsorption isotherms at 77K were collected on a Micromeritics ASAP 2020 HD instrument. Before the analysis, the samples were left overnight at 130°C under vacuum. The surface area (m^2/g) was calculated from the nitrogen adsorption branch of the nitrogen adsorption isotherm at 77K, according to Brunauer–Emmett–Teller (BET) and Langmuir models. The total pore volume V_{tot} (cm^3/g) was calculated from the nitrogen isotherms by NLDFT method and carbon slit pore model up to $p/p^0 = 0.98$. The micropore volume was calculated at $p/p° = 0.1$.

CO_2 and N_2 adsorption isotherms at 298 and 273K and up to 10 bar were collected on a Micromeritics ASAP 2050 instrument. Before the analysis, the samples were left overnight at 130°C under vacuum.

Methane Isotherms. CH_4 sorption measurements at high pressure were performed to test the maximum gas capacity and to determine the isotherm profile from low to high pressures (up to 180 bar), i.e. in a wider range than is usual. This yields the 'deliverable gas' potential of the materials. The experiments were performed using a Micromeritics High Pressure Volumetric Apparatus (HPAV II), equipped with a pressure-booster compressor. Typically used were: 1 g samples obtained by the Friedel Crafts alkylation reaction and, in the case of the Yamamoto-type reaction, 300 mg samples. Before the analysis, the samples were activated overnight at 130°C under vacuum, directly in the steel jar. Each experiment was performed by applying an adsorption-desorption cycle up to 180 bar at 25°C.

RESULTS AND DISCUSSION

Synthesis and structure. A series of porous organic materials were prepared by linking monomers which typically contain two or more aromatic rings linked in a π-covalent system e.g. porphyrin and hexaphenylbenzene, or fused aromatic rings such as carbazole groups and polyacenes.

The multiple reaction sites on the aromatic rings provide a tendency for cross-linking. Moreover, the 3D geometry of the monomers, combined with the formation of carbon-carbon cross-links, favored poorly-packed arrangements of the framework. In fact, the molecular shape of the monomers, which is generally retained within the individual monomeric units in the cross-linked polymeric framework, contribute to the formation of low density structures. Figure 1 shows the cross-linked polymeric frameworks: they include polymers of monomeric units, which were mainly linked by a methylene linker between aromatic rings by the Friedel-Crafts reaction, as well as homo- and co-polymers connected by covalent C-C direct links between aromatic groups.[7,12] In the case of Friedel-Crafts alkylation reaction, the use of FDA and the maintenance of a constant stoichiometry of both FDA and catalyst with respect to each aromatic ring in the monomer unit was applied (1 phenyl ring : 2 FDA : 2 catalyst), resulting in an advantage for a systematic comparison of the results.

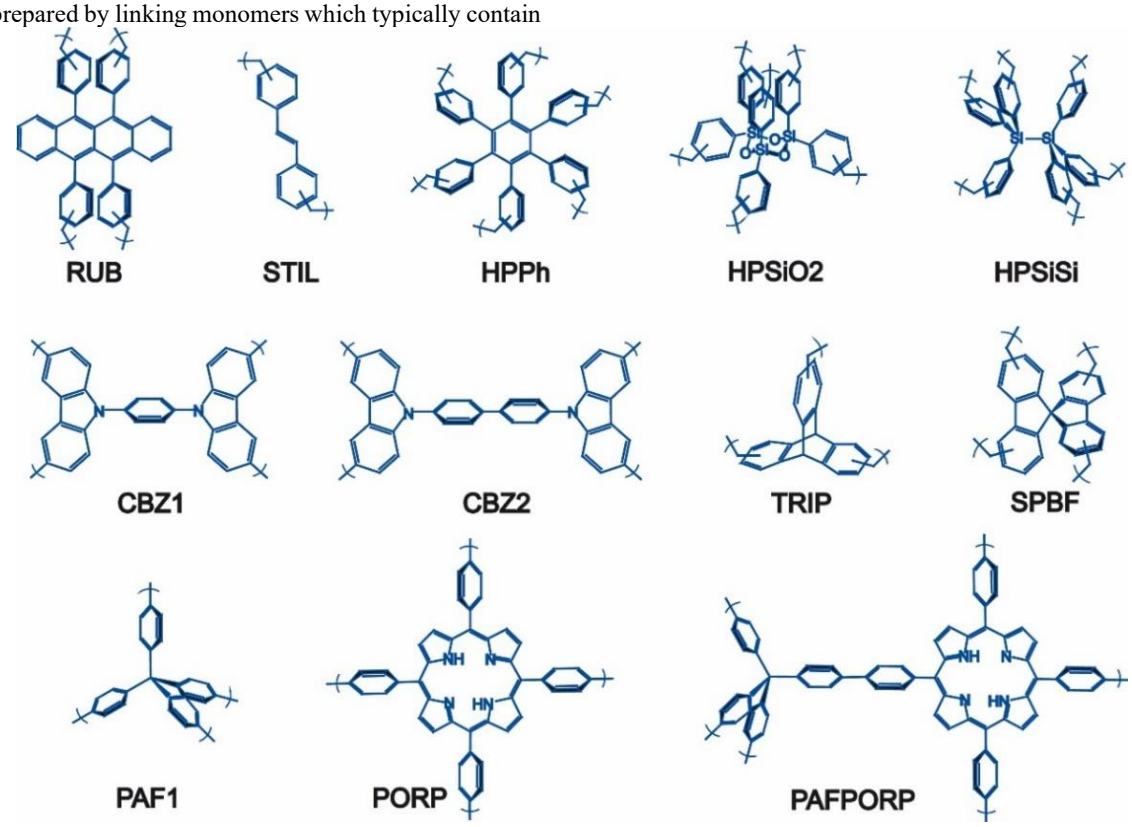

Figure 1. Chemical structures of the microporous 3D polymers. The acronyms of the polymers are reported below the monomer units.

Elemental analysis of the porous polymers by the Yamamoto-type reaction indicated the absence of residual bromine. In the case of copolymers of porphyrin and tetraphenylmethane monomers (PAFPORP), the analysis enabled us to determine the stoichiometry of resulting network (23/77 mole/mole, respectively). FTIR spectra of the porous polymers obtained by Friedel-Craft alkylation reaction revealed the structural features: in particular, owing to the effect of cross-linking, vibrations at 2800-3000 cm^{-1} characteristic of asymmetric and symmetric C-H stretching are observed, revealing that the networks are linked by CH_2 groups (Figures S14-S23). The spectra show a band at about 1700 cm^{-1}, typical of hypercross-linked aromatic systems. Thermogravimetric analysis demonstrated the stability of these porous materials up to or more than 500°C, while powder X-ray diffraction patterns show no defined peak, suggesting the structural disorder of the networks (Figures S1-S13).

The structural investigation at the molecular level was performed by 1D ^{13}C and 2D ^{1}H-^{13}C NMR spectroscopy. The spectra of the porous polymers obtained by both synthetic routes

show resonances between 110 and 150 ppm assigned to the aromatic moieties of monomeric units (Figure 2).[13] No resonances were present in the alifatic region for the frameworks obtained by Yamamoto-type reaction, except in the case of PAF1, which possesses the quaternary sp^3 carbon at the core of the monomeric unit (Figure 2g-l).

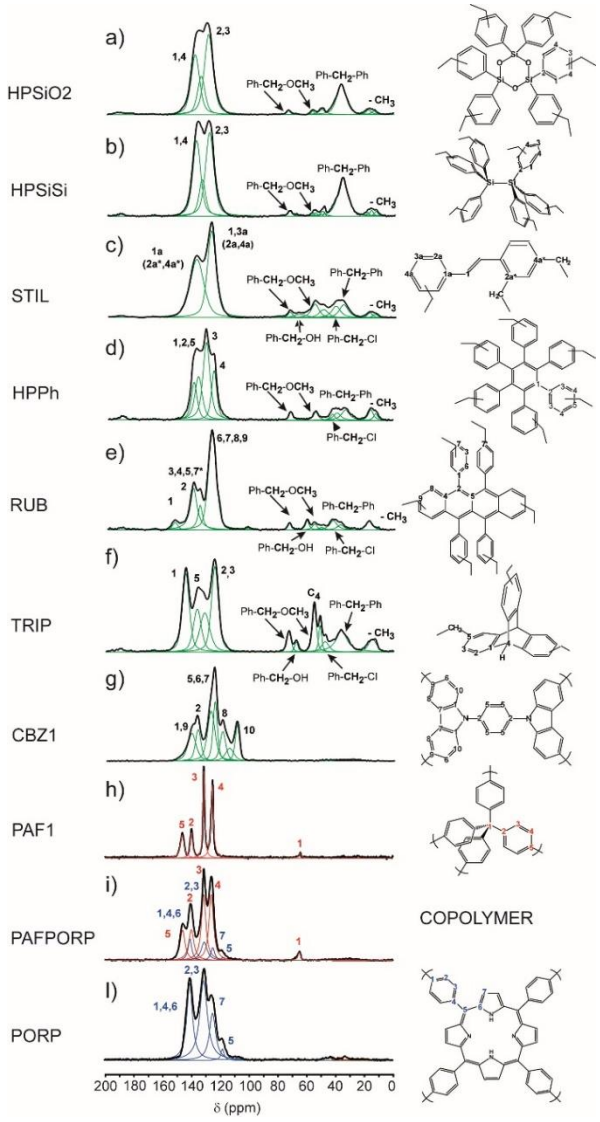

Figure 2. ^{13}C CP MAS NMR spectra of a) HPSiO2, b) HPSiSi, c) STIL, d) HPPh, e) RUB, f) TRIP, g) CBZ1, h) PAF1, i) PAFPROP and l) PORP.

On the opposite, additional signals appear in the aliphatic region for Friedel-Crafts reaction polymers, indipendently of the monomer,. The pattern is complex, because of multiple alkylation reactions of the aromatic rings. The connectivity in the framework was inferred by 2D NMR spectra, which through nuclear dipole-dipole interactions, highlighted the correlation between carbon and hydrogen nuclei in close spatial proximity, providing for the first time in this category of compounds, evidence of the insertion of connecting bridges and pendant groups.[14] Figure 3 reports the 2D MAS spectrum of triptycene-based porous polymer (TRIP): the aromatic hydrogens of the main architecture δ = 6.6 ppm are in correlation with the carbons of the methylene groups (δ = 36.3 ppm)[18] that bridge aromatic paddles of connected monomer units and, *vice versa*, the benzylic CH_2-bridge hydrogens at δ = 4.9 ppm, communicate with the aromatic substituted carbons, unambiguously showing the phenylene groups to be covalently bonded to the CH_2 linkers. Also, CH_2-O carbons of the pendant groups reside at short distance with respect to the aromatic hydrogens (δ_H=6.6-δ_C=72.8 ppm cross-peak), demonstrating they are directly substituted to the aromatic rings through a carbon–carbon bond. By a quantitative analysis of the MAS spectrum obtained with a long recycle delay of 60 s, we could extrapolate the abundance of the linking connectors created by our synthetic procedure using Friedel-Crafts reaction.

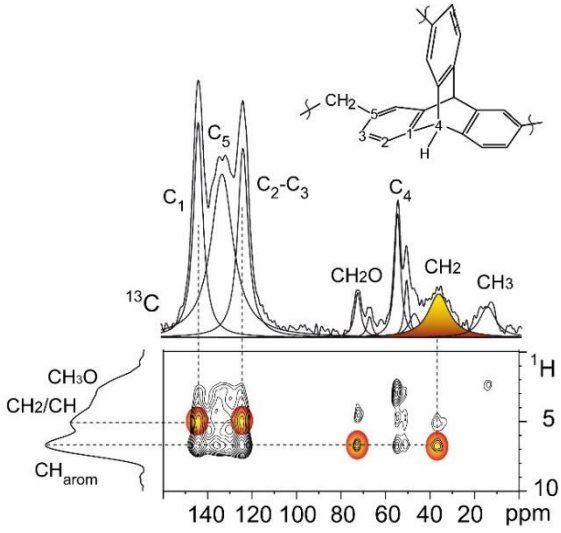

Figure 3. 2D ^1H-^{13}C HETCOR NMR spectra with Lee–Goldbourg decouling of TRIP. The cross-peaks between hydrogens and carbons are highlighted. In ^{13}C dimension the MAS NMR spectrum with recycle delay of 60 s is reported.

N_2 adsorption at 77K. The porosity of the frameworks was tested by N_2 adsorption isotherms at 77 K, which exhibited BET surface areas ranging typically from 1000 to 1700 m^2/g and up to 4800 m^2/g for structures containing tetraphenylmethane as the monomer unit (Figure 4 and Figures S27-S30). The N_2 adsorption isotherms exhibit, in most cases, a steeply sloping gas uptake at relatively low pressures and a continuous rise at higher pressures, reflecting the presence of micro/mesopore distribution (Figure 4). Pore size distribution was calculated by NLDFT method and carbon slit pore model (Figures S31 and S32): Table 1 displays the total pore volumes. The limit cases are the carbazolyl-based compound (CBZCH2) obtained by Friedel-Craft alkylation reaction, which displays a main peak with a diameter smaller than 10 Å, and the stilbene-based (STIL) and hexaphenyldisilane-based (HPSiSi) polymers with pores mainly centered on larger diameters from 10 to 100 Å.

A large hysteresis is observed in many cases between the adsorption and desorption branches, as is mostly evident in CBZ1, CBZ2, TRIP, RUB, STIL, HPSiSi and PAFPORP. The desorption curve closes only at partial pressures around null point. The hysteresis loop in the isotherm is consistent with the swelling of

the network during sorption: an indication of a flexible structure with expandable pores, because capillary condensation in the mesopores causes some strain in the network, as systematically observed in soft polymeric materials.[9]

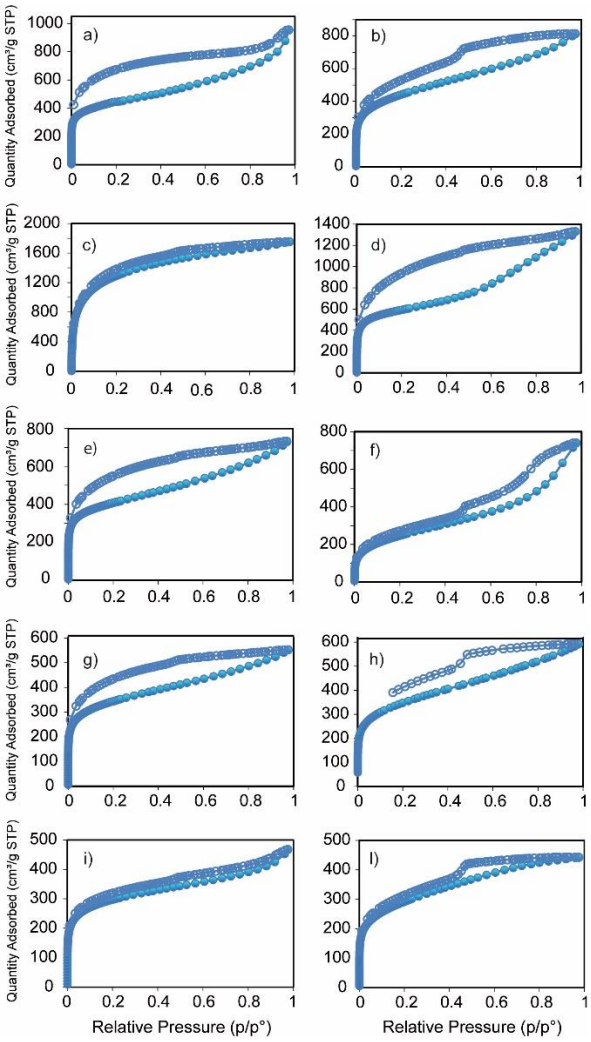

Figure 2. N_2 isotherms collected at 77K of a selection of porous polymers: a) CBZ1, b) TRIP, c) PAF1, d) PAFPORP, e) PORP, f) HPSiSi, g) RUB, h) STIL, i) HPPh and l) HPSiO2.

Table 1. Brunauer-Emmet-Teller and Langmuir surface areas, total pore volume (T.P.V.), micro/total pore volume ratio (M./T. ratio) and decomposition temperature (Dec.T.).

Sample	BET m^2/g	Langmuir m^2/g	T.P.V. cm^3/g	M./T. ratio	Dec.T. K
PAF1[a)]	4784	5485	2.70	0.63	500
PAFPORP	2194	2492	2.02	0.42	400
CBZ2[b)]	1698	1942	1.42	0.46	550
CBZ1	1622	1834	1.40	0.44	550
TRIP[c)]	1592	1895	1.20	0.50	500
PORP[d)]	1494	1703	1.13	0.50	400
SPBF[e)]	1418	1612	0.93	0.53	450
STIL	1254	1525	0.92	0.52	500
RUB	1258	1428	0.85	0.56	500
HPPh	1082	1284	0.72	0.58	450
CBZCH2[f)]	1090	1250	0.53	0.79	450
HPSiO2	1054	1256	0.69	0.58	450
HPSiSi	872	1004	1.15	0.32	500

a) ref. n. 15. b) ref. n. 16. c) ref. 9. d) ref. 17. e) ref. 18. f) ref. 19.

Gravimetric CH_4 adsorption isotherms. Thanks to the large surface area, pore volume and large contribution of the mesopores, porous organic polymers were selected as potentially adsorptive materials for methane storage, especially at high pressures. The polymers were tested experimentally in a wide range of high pressure conditions up to 180 bar, all measurements being taken three times to check the reproducibility of the data (Figure 5a). In CH_4 isotherms it is possible to observe an increasing uptake over the whole range of pressures, although the slope diminishes at high pressures. At 180 bar adsorption values up to 445 cm^3 STP/g (0.32 g/g) were measured for porous organic polymers endowed with surface areas of more than 1600 m^2/g, such as carbazolyl-based (CBZ1 and CBZ2) and triptycene-based (TRIP) materials. Such uptake value is far above the HKUST-1 performance at the same pressure.

Since these high pressure conditions above 100 bar are not frequently reported in the literature, we compared our results at lower pressures with those published. Under the conditions of 65 bar and 298 K the porous polymers CBZ1, CBZ2 and TRIP adsorb a CH_4 amount of 255.4, 252.8 and 240.4 cm^3 STP/g, corresponding to 0.18, 0.18 and 0.17 g/g, respectively. Such high values are comparable with or beyond the CH_4 uptake of COF-5 (0.11 g/g), COF-8 (0.11 g/g), PPN-2 (0.14 g/g), PPN-3 (0.19 g/g), PPN-13 (0.18 g/g) and NiMOF-74 (0.15 g/g).[20,21] At 100 bar the amount of methane adsorbed of CBZ1 (0.23 g/g), CBZ2 (0.23 g/g) and TRIP (0.22 g/g) overcome MOF-5 (0.28 g/g), Mg_2(dobdc) (0.19 g/g) and PCN-14 (0.22 g/g).[3] Carbazolyl-based porous polymers required Nickel-catalyzed coupling reactions (Yamamoto-type reaction) limiting the synthesis of these materials to small scales while the triptycene-based porous polymer was obtained with the cheap catalysts such as $FeCl_3$ and in high yields, making this material suitable for applications.

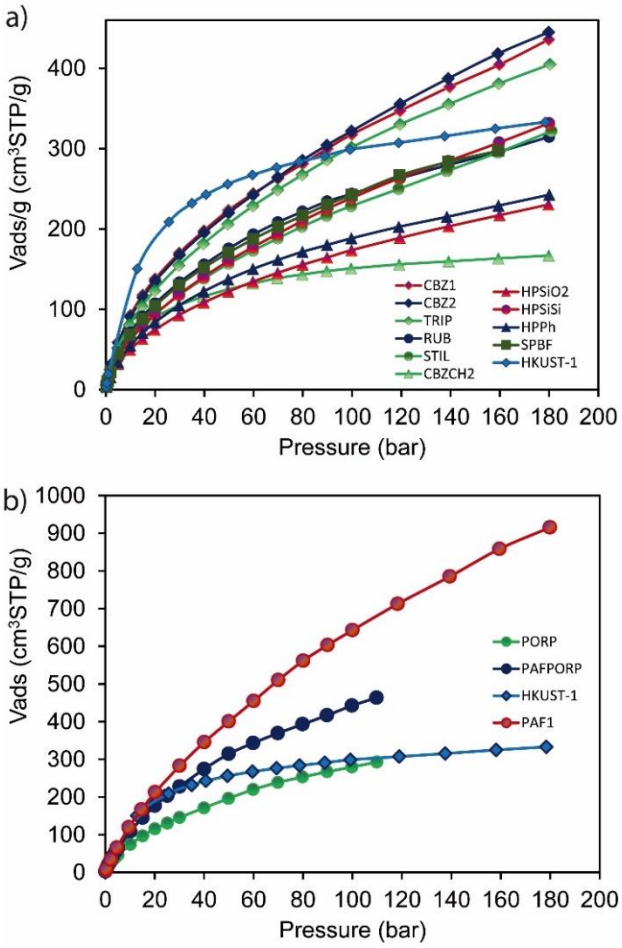

Fig. 5 CH_4 adsorption isotherms collected at 298K of a) porous polymers up to 180 bar and b) PAF1, PAFPOR and PORP as compared to HKUST-1.

In general, the maximum CH_4 absorption values are related to the surface area and pore capacity obtained by nitrogen at 77K, in fact, lower adsorption values of 322 and 242 cm^3 STP/g were observed in the porous materials with surface areas of about 1250 and 1050 m^2/g, respectively. The only exception is hexaphenyldisilane-based (HPSiSi) compound which, despite the low surface area of 872 m^2/g, absorbs up to 332 cm^3 STP/g owing to the large mesoporosity/macroporosity and the relatively large total pore capacity of 1.15 cm^3/g. This is mainly derived by the geometry of the monomer in which six *p*-phenyl groups protrude from the Si-Si moiety, producing 3D nodes that form a complex branching system. The carbazolyl-based porous polymer as synthesized by Friedel Craft alkylation (CBZCH2), exhibits a behavior different from that of the homologue porous polymers obtained by Yamamoto-type reaction, in fact in CBZCH2 a type-I profile is observed, reaching a limit value of 168 cm^3 STP/g at 180 bar: the CH_4 isotherm shape mirrors the Langmuir profile of N_2 adsorption isotherm and the presence of an intense peak in the ultramicropore region.

The benchmark of these materials PAF1 reaches the value of 916 cm^3 STP/g of adsorbed CH_4 at 180 bar (Figure 5b), owing to its high surface area (4800 m^2/g) and pore volume (2.7 cm^3/g). The extremely high methane uptake, corresponding to 65% by weight, represents one of the top values in gravimetric absorptive materials at room temperature. The comparison with HKUST-1 allowed us to show that HKUST-1 saturates at 30-40 bar: at such pressure it shows comparable performances, but much more absolute amount of methane is stored in PAF1 at high pressures, proving the enormous relevance to explore high pressure range. Already at 100 bar PAF1 adsorbs 643 cm^3 STP/g (0.46 g/g) overcoming most of best performing MOFs (HKUST-1, PCN14, MOF-5),[3] COFs (COF-102 and COF-103)[21] and carbon (AX-21 and LMA738)[4,22]. The tetraphenylporphyrin-based porous polymer shows 294 cm^3 STP/g of adsorbed CH_4 at 110 bar, while the copolymer containing both tetraphenylmethane and tetraphenylporphyrin monomeric units, PAFPORP, displays an intermediate absorption value (464 cm^3 STP/g), which is a competitive value and is in agreement with the pore capacity of the material (2.02 cm^3/g). The isotherms are fully reversible, as observed by the coincidence of adsorption and desorption branches, and are reproducible over several cycles (Figure S34), thanks to the high stability of the materials.

Table 2. Amount of methane adsorbed Q (cm^3 STP g^{-1}) by porous polymers at 100 bar and 180 bar.

Sample Name	Q (100 bar) (cm^3 STP g^{-1})	Q (180 bar) (cm^3 STP g^{-1})
PAF1	643	916
PAFPORP	443	n.d.
CBZ1	318	436
CBZ2	328	452
TRIP	300	400
PORP	280	n.d.
RUB	247	290
SPBF	240	289
HPSiSi	240	332
STIL	230	322
CBZCH2	228	167
HPPh	189	242
HPSiO2	175	230

The isosteric heat of adsorption, as measured by Clausius-Clapeyron equation and based on the adsorption values of 273K and 298K, is from 19 up to 21 kJ/mol at low coverage for the various samples (Figure S43). These values are quite notable and match, or go beyond, the performance of MOF: i.e. Ni-MOF-74 (21.4 kJ/mol), PCN-14 (18.7 kJ/mol) and HKUST-1 (17 kJ/mol).[3,20] Such high values indicate that the electron rich aromatic rings play a decisive role in methane adsorption even in the absence of active metal sites. They confirm values found in other porous aromatic frameworks[7] and are attributed to multiple CH - π interactions of CH_4 with aromatic rings,[23] densely populated in this family of polymer frameworks.

Volumetric CH_4 adsorption isotherms. There is also a general desire to store or transport the largest amount of gas per tank available volume. Obviously, medium-high pressures help increase storage, but there has been little experimental testing

of the practical gain obtained with an efficient absorbent at high pressures, nor of the appropriate gas compression needed to obtain the maximum gain for the various materials. These desiderata are valid for any to-be-stored or transported gas, from the automotive area to CNG. The volumetric uptake allowed us to compare the results directly with compressed natural gas technology for naval transportation where volume, and not weight, is the critical issue.

The density of porous polymers plays a key role in the determination of volumetric gas uptake. Since the porous polymers presented here do not show crystalline order, a valuable method to determine the specific volume occupied by the material is based on pore volume (known by N_2 adsorption at 77K), combined with direct density measurement of the framework walls by He picnometry. Indeed, the CH_4 uptake values per matrix volume (Figure 6a) reveal a behavior that, in most cases, attenuates the performance differences previously observed.

Most of MOFs exhibit a large absorption capacity up to about 80 bar, after which saturation occurs. Instead, the CH_4 isotherms of the studied porous polymers reveal that on increasing the pressure to higher values than 100 bar there is a continuous gain in the absorbed amounts. This feature results in a high total volumetric uptake capacity, due to the remarkable contribution of mesoporosity at pressures as high as 180 bar. Furthermore, in such porous polymers, the slope of CH_4 adsorption isotherms is moderate at low pressure, which is a great advantage for a high working capacity, e.g. the amount of deliverable methane taken into account the practical discharge pressure, which can be of several atmospheres to feed the pipelines.

The total volumetric uptake of PAF1 measured at 110 bar is of 198 cm^3STP/cm^3 and is comparable with the values measured for MOF-5 and MOF-210, although the latter exhibits a higher surface area (Figure 6a).[24] At higher pressure (180 bar) the CH_4 uptake reaches the notable value of 266 cm^3 STP/g. On comparing the total volumetric uptake of CH_4 in the presence of PAF1 there is, with respect to pure compressed methane, a maximum gain of an extra 110% at 70 bar. Collectively, most compounds of the family showed considerable volumetric uptake, although less capacitive, than PAF1, consistently with their density, which is a critical parameter for volumetric uptake (Figure 6b).

The porous aromatic polymers are shape-persistent networks as shown by their high mechanical stability. This was demonstrated experimentally by mechanical compression, at a pressure of 9000 psi (620 bar), of the said porous materials and the registration of the CH_4 isotherms after release of mechanical compression. The reduction of storage capacity was less than 8%, consistent with the reduction of pore capacity measured by N_2 adsorption isotherm at 77K (Figure S33). This result demonstrates the scare tendency to close-packing, owing to the intrinsic shape factor of the monomeric units that, had they been able to close-pack, would have resulted in reduced efficiency. The bridges realized to link the monomers through C-C or C-CH_2-C covalent bond contributed to the creation of cross-linked polymeric frameworks, that preserve their porosity after releasing compression.

The present paper is the first report on the experimental screening of CH_4 uptake in the wide pressure range up to 180 bar in investigating the behavior of this class of materials. Indeed, the absorption properties of these porous polymers, together with their thermal stability up to 450-500°C, their chemical inertia, especially towards acidic components and water, their scalable synthesis and low-cost catalysts, make these materials highly competitive for gas storage.

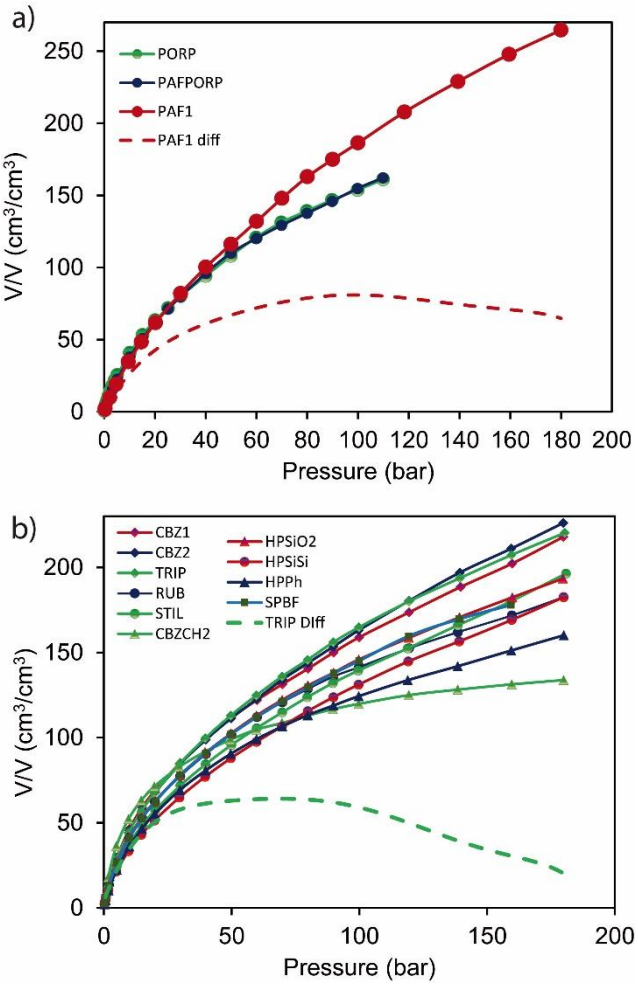

Figure 6. CH_4 adsorption isotherms of a) PAF1, PAFPORP and PORP and b) porous polymers at room temperature and up to 180 bar. The value of total absorption volume over volume is reported versus pressure. The dashed lines represent the difference between the total adsorption value and the pure compressed CH_4.

CO_2 adsorption isotherms. The porous materials under investigation exhibit a high CO_2 capacity, as shown by the CO_2 isotherms at room temperature and up to 10 bar (Figure 7a). The CO_2 uptake values of 183, 174, 162 and 150 cm^3 STP/g are found for the porous polymers CBZ1, CBZ2, TRIP and PORP, respectively, overcoming the performances of zeolite 13X (150 cm^3/g), ZIF-8 (78.4 cm^3/g) and HKUST-1 under the same conditions and active carbons (46 cm^3/g a 22 bar).[9,21,25] Within the present series of aromatic compounds, the stored amount is substantially proportional to the surface area and pore volume. At 10 bar, the slope of the isotherms is still positive, indicating that the porous materials are not yet saturated by CO_2. PAF1 and its copolymer with porphyrin are far more efficient than the other matrices (Figure 7b). Actually, PAF1 shows a benchmark adsorption value: under the relatively mild

conditions of room temperature and 10 bar it reaches 524 mg/g (11.9 mmol/g), such high value outperforms the best representatives of MOFs (MOF-177, MOF-205 and MOF-5), and is comparable to PPN-4.[21,26]

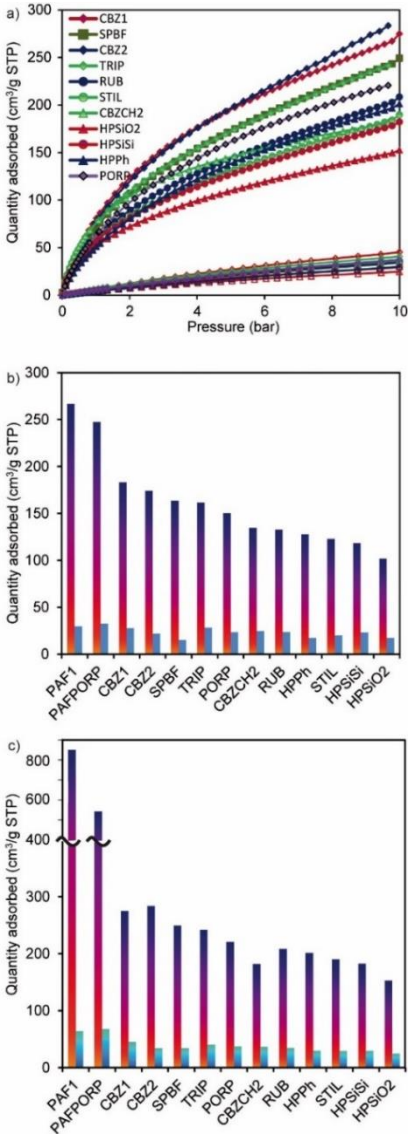

Fig. 7 a) CO_2 and N_2 adsorption isotherms (filled and open labels, respectively) of the porous polymers at 298 K. b) Absolute adsorption at 10 bar of CO_2 (red) and N_2 (light blue) at 298K (b) and 273K (c).

Moreover, reducing the temperature by only 25K, from ambient temperature to 273K, uptake increases by a 50% for the majority of the samples, while a dramatic gain is achieved at 273K and 10 bar by PAF1 (Figure 7b and c). The high CO_2 adsorption value of 1672 mg/g (38 mmol/g) obtained by PAF1, under the said pressure/temperature conditions, is far higher than the values of activated carbon AC-Maxsorb.[26] At 195K and 1 bar PAF1 absorbs 2596 mg/g of CO_2, equal to 1322 cm^3/g and 59 mmol/g, that is far higher than the best recently proposed CO_2 absorbent materials.[26]

The isosteric heat of absorption at low coverage, determined by the Clausius-Clapeyron equation, is quite high, ranging from 24.8 to 29.6 kJ/mol. Interestingly, the CBZCH2 sample, obtained by Friedel Crafts alkylation, exhibits a higher heat of adsorption of 29.0 kJ/mol, than that of compound CBZ2, which was derived by condensation of the same monomer with Yamamoto reaction (25.2 kJ/mol). This was due to the relevant presence of small microporosity in CBZCH2.[27] The CO_2 interaction with the surfaces could have been augmented by oxygen–containing pendant groups, such as CH_2-OH and CH_2-O-CH_3 groups originated by the FDA reagent and revealed by MAS NMR.

Consistently, the TRIP sample, prepared by Friedel Crafts alkylation reaction and containing the highest number of pendant groups shows the highest isosteric heat of adsorption (29.6 kJ/mol). A value of about 30 kJ/mol is considered to be an optimal balance between an effective uptake and a convenient release by a porous framework.[28] The covalent organic polymers do not contain bonds susceptible to hydrolysis. Indeed, polymer stability towards water, water being a frequent contaminant of CO_2 streams, is a general advantage over most MOFs, which are water sensitive.

The porous polymers are poor absorbers of N_2, compared to CO_2 absorption at the same temperature (see Fig. 7b and c at 298K and 273K, respectively). Indeed, the adsorption selectivity in favor of CO_2 with respect to other components is influenced by several factors including the geometry of the pores (size and shape) and energy interaction between the gases and pore walls. The porous materials exhibit excellent CO_2/N_2 selectivity (S) at low pressure (estimated by Ideal Adsorbed Solution Theory IAST) ranging from 15 to 25 at room temperature (starting from a 15:85 CO_2:N_2 mixture), and the selectivity values are weakly dependent on pressure. Such values are higher than those reported for activated carbon BPL AC (S=20-26 at 1 bar), zeolite 13X (S=18 at 1bar and S=3 at 10 bar) and ZIF-8 (S=7.6-8.4 at 1 bar),[25,29] opening perspectives for applications to post-combustion treatment of industrial polluting emissions.

CONCLUSIONS

The experimental screening comprises gravimetric and volumetric gas uptake by the frameworks obtained by 3D polymerization or condensation of various monomers with increasing number of phenyl, phenylene, carbazole rings and acenes in a unique unitary frame. Indeed, a large variety of highly absorptive polymers and copolymers were produced by combining possibly the use of commercially-available low-cost monomers and Friedel-Crafts alkylation, a robust reaction, scalable to industrial purposes. Primarily 2D MAS NMR spectroscopy recognized multiple short methylene and longer alkyl bridges per monomer unit which result in the construction of flexible porous 3D networks. These materials provide a suitable surface wall-to-pore volume balance and adsorption energies for optimizing high-pressure methane storage, paving the way to future developments in gas storage. The present results demonstrate that virtually all aromatic precursors with multiple connected aromatic groups can be condensed, and a few of them are suitable as precursors to form benchmark materials in the competition for loading efficiently methane and carbon dioxide. We suggest that these metal-free nanoporous materials realize an optimal compromise, given their advantageous operative properties and their cost.

ASSOCIATED CONTENT

Supporting Information

Experimental details, thermocalorimetric analysis, MAS NMR spectroscopy, gas adsorption measurements (PDF). The Supporting Information is available free of charge on the ACS Publications website.

AUTHOR INFORMATION

Corresponding author

Email: *piero.sozzani@mater.unimib.it,
Email: *angiolina.comotti@mater.unimib.it

ACKNOWLEDGMENT

Cariplo Foundation 2016, PRIN 2016-NAZ-0104 and IN-RL14-2016 are acknowledged for financial support. The authors would like to thank G. Sormani for helpful discussion.

REFERENCES

(1) (a) Thomas, S.; Dawe, R. A. *Energy* **2003**, *28*, 1461. (b) Faramawy, S.; Zaki, T.; Sak, A.A.-E. *J. Nat. Gas Sci. Eng.* **2016**, *34*, 34.

(2) (a) Economides, M. J.; Wood, D. A. *J. Nat. Gas Sci. Eng.* **2009**, *1*, 1. (b) Choi, P.-S.; Jeong, J.-M.; Choi, Y.-K.; Kim, M.-S.; Shin, G.-J.; Park, S.-J. *Carbon Lett.* **2016**, *17*, 18.

(3) (a) Mason, J. A.; Veenstra, M.; Long, J. R. *Chem. Sci*. **2014**, *5*, 32. (b) Dawson, R.; Cooper, A. I.; Adams, S. J. *Progr. Polym. Sci.* **2012**, *37*, 530. (c) Saha, D.; Bao, Z.; Jia, G.; Deng, S. *Envir. Sci. Technol.* **2010**, *44*, 1820. (d) Kitagawa, S.; Kitaura, R.; Noro, S.-I. *Angew. Chem. Int. Ed.* **2004**, *43*, 2334. (e) Horike, S.; Shimomura, S.; Kitagawa, S. *Nature Chem.,* **2009**, *1*, 695.

(4) (a) Li, B.; Wen, H.-M.; Zhou, W.; Xu, J. Q.; Chen, B. *Chem*, **2016**, *1*, 557. (b) Makal, T. A.; Li, J.-R.; Lu, W.; Zhou, H.-C. *Chem. Soc. Rev.* **2012**, *41*, 43. (c) Menon, V. C.; Komarneni, S. *J. Porous Mater.* **1998**, *5*, 43. (d) A. Del Regno, A. Gonciaruk, L. Leay, M. Carta, M. Croad, R. Malpass-Evans, N. B. McKeown and F. R. Siperstein, *Ind. Eng. Chem. Res*., **2013**, *52*, 16939.

(5) (a) Barin, G.; Krungleviciute, V.; Gomez-Gualdron, D. A.; Sarjent, A. A.; Snurr, R. Q.; Hupp, J. T.; Yildirim, T.; Fahra, O. K. *Chem. Mater.* **2014**, *26*, 1912. (b) Gandara, F.; Furukawa, H.; Lee, S.; Yaghi, O. *J. Am. Chem. Soc.* **2014**, *136*, 5271. (c) Li, B.; Wen, H.-M.; Wang, H.; Wu, H.; Tyagi, M.; Yildirim, T.; Zhou, W.; Chen, B. *J. Am. Chem. Soc.* **2014**, *136*, 6207.

(6) (a) Schoenecker, P. M.; Carson, C. G.; Jasuja, H.; Flemming, C. J. J.; Walton, K. S. *Ind. Eng. Chem. Res.* **2012**, *51*, 6513.

(7) (a) Qiu, S.; Ben, T. *Porous Polymers: Design, Synthesis and Applications*, Royal Society of Chemistry: Cambridge, 2015. (b) Ben, T.; Ren, H.; Ma, S. Q.; Cao, D. P.; Lan, J. H.; Jing, X. F.; Wang, W. C.; Xu, J.; Deng, F.; Simmons, J. M.; Qiu, S. L.; Zhu, G. S. *Angew. Chem. Int. Ed.* **2009**, *121*, 9621. (c) Xu, S.; Luo, Y.; Tan, B. *Macromol. Rapid Commun.* **2013**, *34*, 471. (d) Ben, T.; Qiu, S. *Cryst. Eng. Comm.* **2013**, *15*, 17. (e) Wood, C. D.; Tan, B.; Trewin, A.; Su, F.; Rosseinsky, M. J.; Bradshaw, D.; Sun, Y.; Zhou, L.; Cooper, A. *Adv. Mater*. **2008**, *20*, 1916. (f) Thomas, A.; Kuhn, P.; Weber, J.; Titirici, M.-M.; Antonietti, M. *Macromol. Rap. Commun.* **2009**, *30*, 221. (g) Mckewon, N.; Budd, P. *Macromolecules* **2010**, *43*, 5163. (h) Chen, Q.; Luo, M.; Hammershoj, P.; Zhou, D.; Han, Y.; Laursen, B. W.; Yan, C.-G.; Han, B.-H. *J. Am. Chem. Soc.* **2012**, *134*, 6084.

(8) Mason, J. A.; Oktawiec, J.; Hudson, M. K.; Rodriguez, J.; Bachman, J. E.; Gonzalez, M. I.; Cervellino, A.; Guagliardi, A.; Brown, C. M.; Llewellyn, P. L.; Masciocchi, N.; Long, J. R. *Nature* **2015**, *527*, 357.

(9) (a) Weber, J.; Antonietti, M.; A. Thomas, A. *Macromolecules*, **2008**, *41*, 2880. (b) Woodword, R. T.; Stevens, L. A.; Dawson, R.; Vijayaraghavan, M.; Hasell, R.; Silverwood, I. P.; Ewing, A. V.; Ratvijitvech, T.; Exley, J. D.; Chong, S. Y.; Blanc, F.; Adams, D. J.; Kazarian, S. G.; Snape, C. E.; Drage, T. C.; Cooper, A. I. *J. Am. Chem. Soc.* **2014**, *136*, 9028. (c) Kowalczyk, P.; Furmaniak, S.; Gauden, P. A.; Terzyk, A. P. *J. Phys. Chem. C* **2012**, *116*, 1740.

(10) (a) Kizzie, A. C.; Dailly, A.; Perry, L.; Lail, M. A.; Lu, W.; Nelson, T. O.; Cai, M.; Zhou, H.-C. *Materials Sciences and Applications* **2014**, *5*, 387. (b) Tong, W.; Lv, Y.; Svec, F. *Applied Energy* **2016**, *183*, 1520. (c) Li, Y.; Ben, T.; Zhang, B.; Fu, Y.; Qiu, S. *Sci. Rep.* **2013**, *3*, 2420. (d) Pei, C.; Ben, T.; Li, Y.; Qiu, S. *Chem. Comm.* **2014**, *50*, 6134. (e) Schwab, M. G.; Lennert, A.; Pahnke, J.; Jonschler, G.; Koch, M.; Senkovska, I.; Rehahn, M.; Kaskel, S. *J. Mater. Chem.,* **2011**, *21*, 2131.

(11) (a) Vinogradov, E.; Madhu, P. K.; Vega, S. *J. Chem. Phys.* **2001**, *115*, 8983. (b) Brown, S. P. *Solid State Nucl. Magn. Reson.* **2012**, *41*, 1. (c) Sozzani, P.; Comotti, A.; Bracco, S.; Simonutti, R. *Chem. Commun.* **2004**, 768. (d) Bracco, S.; Comotti, A.; Ferretti, L.; Sozzani, P. *J. Am. Chem. Soc.* **2011**, *133*, 8982. (e) Sozzani, P.; Bracco, S.; Comotti, A.; Simonutti, R.; Camurati, I. *J. Am. Chem. Soc.* **2003**, *125*, 12881.

(12) Yamamoto, T. ; Wakabayashi, S.; Osakada, K. *J. Organomet. Chem.* **1992**, *428*, 223. (13) (a) Law, R. V.; Sherrington, D. C.; Snape, C. E.; Ando, I.; H. *Macromolecules* **1996**, *29*, 6284. (b) Errahali, M.; Gatti, G.; Tei, L.; Paul, G.; Rolla, G. A.; Canti, L.; Fraccarollo, A.; Cossi, M.; Comotti, A.; Sozzani, P.; Marchese, L. *J. Phys. Chem. C* **2014**, *118*, 28699.

(14) (a) Bracco, S.; Comotti, A.; Ferretti, L.; Sozzani, P. *J. Am. Chem. Soc*. **2011**, *133*, 8982. (b) Yadav, V. N.; Comotti, A.; Sozzani, P.; Bracco, S.; Bonge-Hansen, T.; Hennum, M.; Gorbitz, C. H. *Angew. Chem. Int. Ed*. **2015**, ***54***, 15684. (c) Sozzani, P.; Comotti, A.; Bracco, S.; Simonutti, R. *Angew. Chem. Int. Ed*. **2004**, *43*, 2792.

(15) (a) Li, Y.; Ben, T.; Zhang, B.; Fu, Y.; Qiu, S. *Scientific Reports*, **2013**, *3*, 2420. (b) Comotti, A.; Bracco, S.; Ben, T.; Qiu, S.; Sozzani, P. *Angew. Chem. Int. Ed*. **2014**, *126*, 1061. (c) Comotti, A.; Bracco, S.; Mauri, M.; Mottadelli, S.; Ben, T.; Qiu, S.; Sozzani, P. *Angew. Chem. Int. Ed*. **2012**, *51*, 10136.

(16) Yang, X.; Yao, S.; Yu, M.; Jiang, J.-X. *Macromol. Rapid Comm.* **2014**, *35*, 834.

(17) Li, B.; Guan, Z.; Yang, X.; Wang, W. D.; Wang, W.; Hussain, I.; Song, K.; Tang, B.; Li, T. *J. Mater. Chem. A* **2014**, *2*, 11930.

(18) (a) Modak, A.; Maegawa, Y.; Goto, Y.; Inagaki, S. *Polym. Chem.,* **2016**, *7*, 1290. (b) Schmidt, J.; Werner, M.; Thomas, A. *Macromolecules* **2009**, *42*, 4426.

(19) (a) Zhang, X.; Lu, J.; Zhang, J. *Chem. Mater.* **2014**, *26*, 4023.

(20) (a) Penag, Y.; Krungleviciute, V.; Eryazici, I.; Hupp, J. T.; Farha, O. K.; Yildirim, T. *J. Am. Chem. Soc.* **2013**, *135*, 11887. (b) Hulvey, Z.; Vlaisavljevich, B.; Mason, J. A.; Tsivion, E.; Dougherty, T. P.; Bloch, E. D.; Head-Gordon, M.; Smit, B.; Long, J. R.; Brown, C. M. *J. Am. Chem. Soc*. **2015**, *137*, 10816.

(21) (a) Furukawa, H.; Yaghi, O. *J. Am. Chem. Soc.* **2009**, *131*, 8875. (b) Lu, W. G.; Yuan, D. Q.; Zhao, D.; Schilling, C. I.; Plietzsch, O.; Muller, M.; Brase, S.; Guenther, J.; Blumel, J.; Krishna, R. et al., *Chem. Mater.* **2010**, *22*, 5964.

(22) Casco, M. E.; Martinez, M.; Gadea-Ramos, E.; Kaneko, K.; Silvestre-Albero, J.; Rodriguez-Reinoso, F. *Chem. Mater*. **2015**, *27*, 959.

(23) (a) Bracco, S.; Comotti, A.; Ferretti, L.; Sozzani, P. *J. Am. Chem. Soc.* **2011**, *133*, 8982. (b) Bracco, S.; Comotti, A.; Ferretti, L.; Simonutti, R.; Sozzani, P. *Angew. Chem. Int. Ed.* **2005**, *44*, 1816. (c) Sozzani, P.; Comotti, A.; Bracco, S.; Simonutti, R. *Angew. Chem. Int. Ed.* **2004**, *43*, 2792. (d) Sozzani, P.; Comotti, A.; Bracco, S.; Simonutti, R. *Chem. Commun.* **2004**, 768. (e) Bracco, S.; Comotti, A.; Valsesia, P.; Beretta, M.; Sozzani, P. *Cryst. Eng. Commun.* **2010**, *12*, 2318.

(24) Furukawa, H.; Ko, N.; Go, Y. B.; Aratani, N.; Choi, S. B.; Choi, E.; Yazaydin, A. O.; Snurr, R. Q., O'Keeffe, M.; Kim, J.; Yaghi, O. M. *Science* **2010**, *329*, 424.

(25) (a) Cavenati, S.; Grande, C. A.; Rodriguez, A. E. *J. Chem. Eng. Data* **2004**, *49*,1095. (b) Liu, D.; Wu, Y.; Xia, Q.; Li, Z.; Xi, H. *Adsorption* **2013**, *19*, 25.

(26) (a) Millward, A. L.; Yaghi, O. M. *J. Am. Chem. Soc.* **2005**, *127*, 17998. (b) Himeno, J. S.; Komatsu, T.; Fujita, S. *J. Chem. Eng. Data* **2005**, *50*, 369. (c) Yuan, D.; Lu, W.; Zhao, D.; Zhou, H. C. *Adv. Mater.* **2011**, *23*, 3723. (d) Lee, J.-S. M.; Briggs, M. E.; Hasell, T.; Cooper, A. I. *Adv. Mater.* **2016**, *28*, 9804.

(27) (a) Comotti, A.; Bracco, S.; Distefano, G.; Sozzani, P. *Chem. Commun.* **2009**, 284. (b) Comotti, A.; Fraccarollo, A.; Beretta, M.; Distefano, G.; Cossi, M.; Marchese, L.; Riccardi, C.; Sozzani, P. *Cryst. Eng. Commun*. **2013**, *15*, 1503. (c) Bassanetti, I.; Comotti, A.; Sozzani, P.; Bracco, S.; Calestani, G.; Mezzadri, L.; Marchio', L. *J. Am. Chem. Soc.* **2014**, *136*, 14883.

(28) Dawson, R.; Cooper, A. I.; Adams, D. J. *Polym. Int.* **2013**, *62*, 345.

(29) McEwen, J.; Hayman, J.-D.; Yazaydin, A. O. *Chem. Phys.* **2013**, *412*, 72.